Turk J Phys
25 (2001) , 563 – 574.

Directional Solidification of Pure Succinonitrile and Succinonitrile- Salol Alloys

İbrahim KARACA, Emin ÇADIRLI, Hasan KAYA
Niğde University, Faculty of Arts and Science, Department of Physics, Niğde - TURKEY
Necmettin MARAŞLI
Erciyes University, Faculty of Arts and Science, Department of Physics, Kayseri-TURKEY
e-mail address: marasli@erciyes.edu.tr.

Received 11.04.2000

Abstract

Pure succinonitrile (SCN) and succinonitrile-salol alloys with four different concentrations of salol were unidirectionally solidified at five different growth rates in a temperature gradient. The microstructure parameters, viz., the primary dendrite arm spacing λ_1, dendrite tip radius R and mushy zone depth d, were measured. The dependence of the microstructure parameters on the solidification parameters for pure SCN and SCN-Salol alloys were determined via linear regression analysis. The results are compared with published data.

Key Words: Organic alloys, directional solidification, microstructure and dendritic growth

1. Introduction

A dendrite structure is the most frequently observed structure when a material is solidified. Dendritic growth may be brought out by imposing either a temperature gradient in a pure materials [1] or a solute gradient in an alloy system [2]. Transparent organic materials have been successfully used for solidification studies by other authors [3-18].

A dendrite structure is characterized by parameters λ_1, λ_2,R and d shown in Figure 1. The solidification variables are the imposed temperature gradient G and growth rate V for directional solidification of pure materials. The solidification parameters are the imposed temperature gradient G, growth rate V and composition of the alloys C_0 for

directional solidification of binary alloys. In directional solidification, the dependency of the solidification parameters on the microstructure parameters are investigated. The microstructure parameters plays an important role in the mechanical properties of metallic materials.

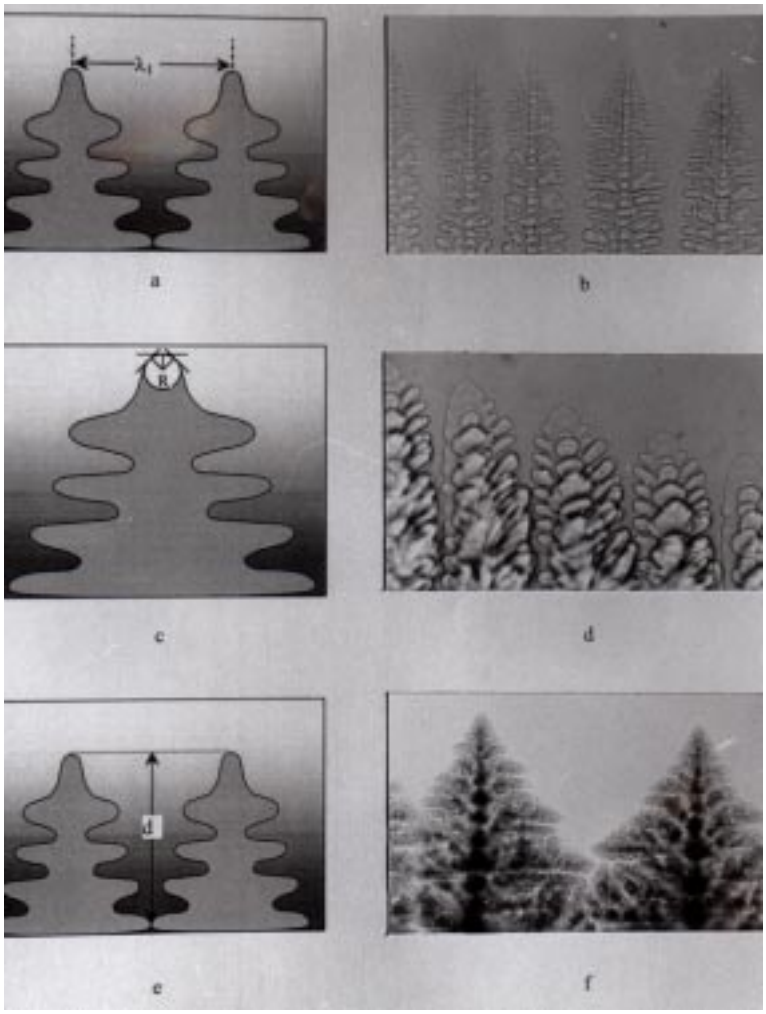

Figure 1. Definition of microstructure parameters (a, b). Schematic and photographic illustration of primary dendrite arm spacing (c, d). Schematic and photographic illustration of dendrite tip radius (e, f). Schematic and photographic illustration of mushy zone depth.

The aim of the present work is to examine the affect of solidification parameters on the microstructure parameters. Pure SCN and SCN-salol alloys having four different

concentrations of salol have been grown unidirectionally in a thin cell to observe the microstructure for five different growth rates in a temperature gradient. The SCN–salol system was chosen for experimental study on account of its "metal-like" freezing behavior and its transparency which permits direct observation of the solid-liquid interface.

2. Experimental Details

In the present work, SCN-salol alloys with four different concentrations of salol were prepared from 99.9 % purity SCN and 99.9 % purity salol supplied by Merck Ltd. The specimen was contained in a glass cell made from two glass cover slips (50 mm long, 24 mm wide and 0.05 mm thick). The slides were placed with their largest surface in the x-y plane and spaced a distance of about 100 μm apart in the z direction. The pure SCN and SCN-salol alloys were solidified in a horizontal directional solidification apparatus to directly observe microstructure in situ using a transmission optical microscope. The details of the apparatus and specimen preparation are given in Ref. [6]. The temperature of the heater was controlled within $\pm$ 0.1 $^{\circ}$C with a Eurotherm 815S type controller. One side of the cell was heated, while the other side of the cell was kept cool with a water cooling system. The temperatures in the specimen were measured with insulated K-type thermocouples, 50 μm thick. As shown in Figure 2, the temperature gradient at the solid-liquid interface on the specimen during the solidification was observed to be constant.

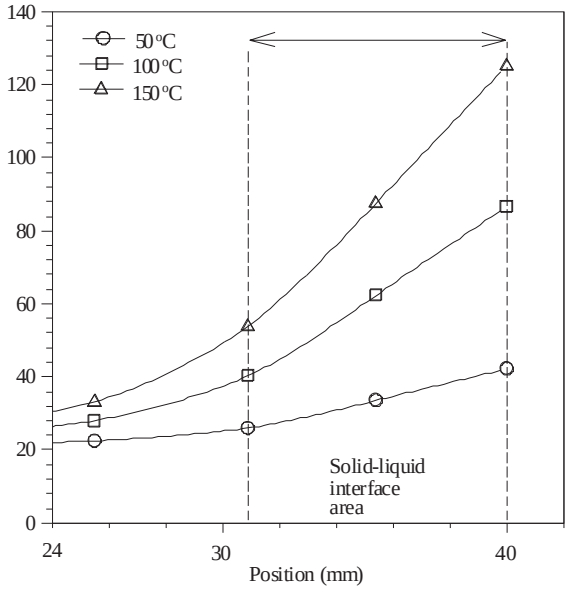

Figure 2. The plot of temperature versus position in the sample.

Driving the specimen cell toward to the heating system the specimen was slowly melted until the solid-liquid interface passed through the second thermocouple (0.05 mm thick K-type). When the solid-liquid interface was between the second and third thermocouple, the synchronous motor was stopped and the specimen was left to reach thermal equilibrium.

3. The Measurement Of Temperature Gradient, Growth Rate and Microstructure Parameters

After the specimen reached steady state conditions, solidification was started by driving the specimen to the cooling system by synchronous motor. As the interface passed between the first and second thermocouples, the solidification time between the two thermocouples Δt and temperature difference between the two thermocouples ΔT were recorded simultaneously with a stopwatch and a Hewlett Packard 34401 A Model multimeter, respectively. The thermocouple positions and solidification microstructure were photographed with an Olympus BH2 light optical microscope using x5, x10, and x20 objectives. A graticule (100 x 0.01 = 1 mm) was also photographed using the same objectives.

Photographs of the thermocouple position and the graticule were projected on graph-paper. Thus the distance between the two thermocouples Δx was measured accurately. The temperature gradient $G = \Delta T / \Delta x$ was calculated by using the values of ΔT and Δx. The growth rates $V = \Delta x / \Delta t$ was also calculated from the values of Δx and Δt. The solidification of the pure SCN and SCN-5, 10, 15 and 20 wt. % salol alloys were carried out for five different growth rates in a temperature gradient. The photographs of the microstructure were taken during the solidification. From the photographs, microstructure parameters, λ_1, R, and d as shown in Figure 1, were measured. Thus the solidification parameters and microstructure parameters were accurately measured and are given in Table 1.

4. Results and Discussion

In the present work, the measurements of the microstructure parameters λ_1, R and d were carried out using about sixty dendrite shapes (Figure 3, 4 and 5). The measured microstructure parameters and their standard deviations are given in Table 1. The relationships between microstructure parameters and the solidification parameters were obtained by linear regression analysis. The results are given in Table 2 and Figure 6. As can be seen from Figure 6, the values of λ_1, R and d decrease exponentially as the value of V increase.

Table 1. Dependence of the microstructure parameters (λ_1, R, d) for different growth rates and compositions.

Composition (wt %)	G (°C/cm)	V(cm/s) x 10^{-4}	GV(°C/s)	λ_1(cm) x 10^{-4}	R (cm) x 10^{-4}	d (cm) x 10^{-4}	λ_1/R	λ_1/d	R/d
Pure Scn	37	183	0.68	157±16	53±3	76±7	2.96	2.07	0.70
		73	0.27	194± 19	73±5	103±11	2.66	1.88	0.71
		42	0.15	217± 21	76±4	186±19	2.86	1.17	0.41
		15	0.05	232± 23	108±6	325±32	2.15	0.71	0.33
		8	0.03	250± 25	121±7	375±38	2.07	0.67	0.32
						Average value:	2.54	1.30	0.49
5wt. % Salol	45	113	0.51	263±27	42±2	219±21	6.26	1.20	0.19
		60	0.27	280±28	52±3	248±25	5.38	1.13	0.21
		34	0.15	327±32	61±4	294±29	5.36	1.11	0.21
		13	0.06	390±38	74±4	419±42	5.27	0.93	0.18
		7	0.03	449±44	87±5	510±51	5.16	0.88	0.17
						Average value:	5.48	1.05	0.19
10wt. % Salol	45	93	0.42	177±18	36±2	181±19	4.92	0.98	0.20
		51	0.23	263± 26	39±2	254±25	6.74	1.03	0.15
		32	0.15	349± 33	64±4	348±35	5.45	1.00	0.18
		15	0.07	422± 41	83±5	623±62	5.08	0.68	0.13
		9	0.04	693± 70	103±6	724±74	6.73	0.96	0.14
						Average value:	5.78	0.93	0.16
15wt.% Salol	69	112	0.76	377± 38	51±3	263±26	7.39	1.43	0.19
		59	0.40	421± 42	54±3	338±34	7.80	1.25	0.14
		31	0.21	582± 57	61±4	447±44	9.54	1.30	0.14
		14	0.10	726± 70	69±4	600±59	10.52	1.21	0.12
		7	0.05	1160± 121	75±5	919±92	15.47	1.26	0.08
						Average value:	10.14	1.29	0.13
20wt. % Salol	26	96	0.25	439±43	54±3	350±36	8.13	1.25	0.15
		57	0.15	533±53	69±4	470±46	7.72	1.13	0.15
		32	0.08	590±58	75±5	596±60	7.87	0.99	0.13
		14	0.04	679±66	87±5	834±83	7.80	0.81	0.10
		7	0.02	787±77	96±6	1289±128	8.20	0.61	0.07
						Average value:	7.94	0.96	0.12

Table 2. Relationships between the structure parameters and solidification parameters.

System	Relationships	Constant (k)	Correlation coefficients (r)
Pure SCN	$\lambda_1 = k_1 V^{-0.14}$	$k_1 = 9.4 \times 10^{-3}$ cm $^{1.14}$ s $^{-0.14}$	$r_1 = -0.97$
	$R = k_2 V^{-0.26}$	$k_2 = 8.5 \times 10^{-3}$ cm $^{1.26}$ s $^{-0.26}$	$r_2 = -0.99$
	$d = k_3 V^{-0.55}$	$k_3 = 0.8 \times 10^{-3}$ cm $^{1.55}$ s $^{-0.55}$	$r_3 = -0.97$
SCN- 5 wt. % Salol	$\lambda_1 = k_4 V^{-0.19}$	$k_4 = 10.6 \times 10^{-3}$ cm $^{1.19}$ s $^{-0.19}$	$r_4 = -0.99$
	$R = k_5 V^{-0.25}$	$k_5 = 1.4 \times 10^{-3}$ cm $^{1.25}$ s $^{-0.25}$	$r_5 = -0.99$
	$d = k_6 V^{-0.31}$	$k_6 = 5.1 \times 10^{-3}$ cm $^{1.31}$ s $^{-0.31}$	$r_6 = -0.99$
SCN- 10wt. % Salol	$\lambda_1 = k_7 V^{-0.39}$	$k_7 = 3.9 \times 10^{-3}$ cm $^{1.39}$ s $^{-0.39}$	$r_7 = -0.93$
	$R = k_8 V^{-0.48}$	$k_8 = 0.3 \times 10^{-3}$ cm $^{1.48}$ s $^{-0.48}$	$r_8 = -0.98$
	$d = k_9 V^{-0.63}$	$k_9 = 1.0 \times 10^{-3}$ cm $^{1.63}$ s $^{-0.63}$	$r_9 = -0.99$
SCN- 15wt. % Salol	$\lambda_1 = k_{10} V^{-0.40}$	$k_{10} = 5.8 \times 10^{-3}$ cm $^{1.40}$ s $^{-0.40}$	$r_{10} = -0.98$
	$R = k_{11} V^{-0.15}$	$k_{11} = 2.6 \times 10^{-3}$ cm $^{1.15}$ s $^{-0.15}$	$r_{11} = -0.99$
	$d = k_{12} V^{-0.44}$	$k_{12} = 3.5 \times 10^{-3}$ cm $^{1.44}$ s $^{-0.44}$	$r_{12} = -0.99$
SCN- 20wt. % Salol	$\lambda_1 = k_{13} V^{-0.21}$	$k_{13} = 17.3 \times 10^{-3}$ cm $^{1.21}$ s $^{-0.21}$	$r_{13} = -0.99$
	$R = k_{14} V^{-0.21}$	$k_{14} = 2.2 \times 10^{-3}$ cm $^{1.21}$ s $^{-0.21}$	$r_{14} = -0.97$
	$d = k_{15} V^{-0.48}$	$k_{15} = 3.8 \times 10^{-3}$ cm $^{1.48}$ s $^{-0.48}$	$r_{15} = -0.99$

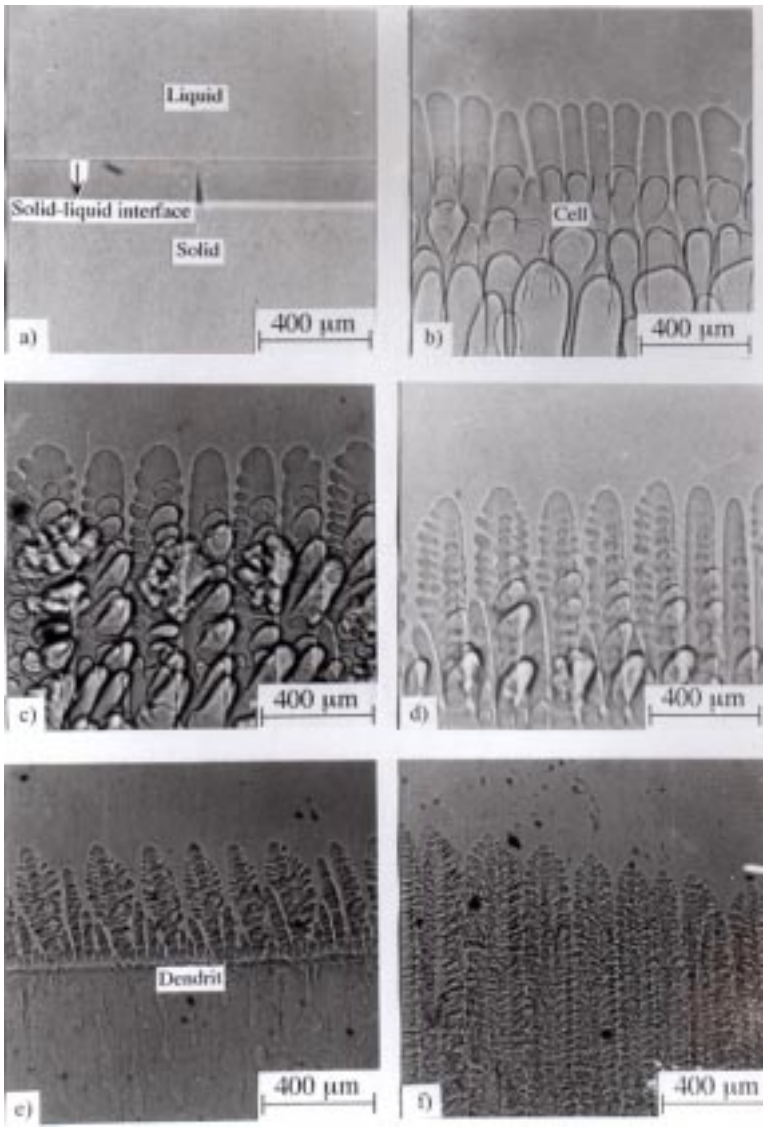

Figure 3. The directional solidification of pure SCN system for increasing growth rates in a temperature gradient (G: 37 $^{\circ}$C/cm) a) Planar form; b) Cellular form; c) Dendritic form, V:42 x10^{-4} cm/s; d) the directional solidification of SCN- 5 wt % Salol system for increasing growth rates in a temperature gradient (G: 45 $^{\circ}$C/cm), V:73 x10^{-4} cm/s; e) V:7 x10^{-4} cm/s; f) V:13 x10^{-4} cm/s.

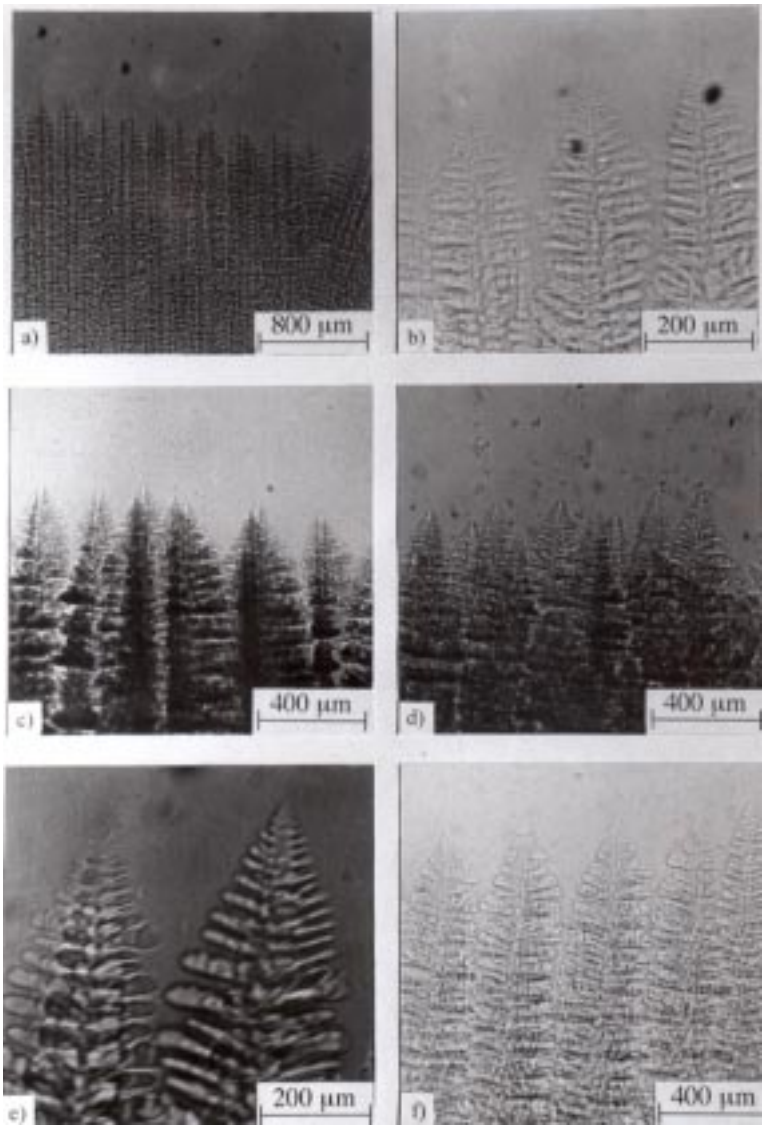

Figure 4. The directional solidification of SCN- 5 wt % Salol system for increasing growth rates in a temperature gradient (G: 45 $^{\circ}$C/cm): a) the directional solidification of SCN-10 wt % Salol system for increasing growth rates in a temperature gradient (G: 45 $^{\circ}$C/cm), V:34 x10^{-4} cm/s; b) V:9 x10^{-4} cm/s; c) V:51 x10^{-4} cm/s; d) the directional solidification of SCN-15 wt % Salol system for increasing growth rates in a temperature gradient (G: 69 $^{\circ}$C/cm) V:93 x10^{-4} cm/s; e) V:7 x10^{-4} cm/s; f) V:14 x10^{-4} cm/s.

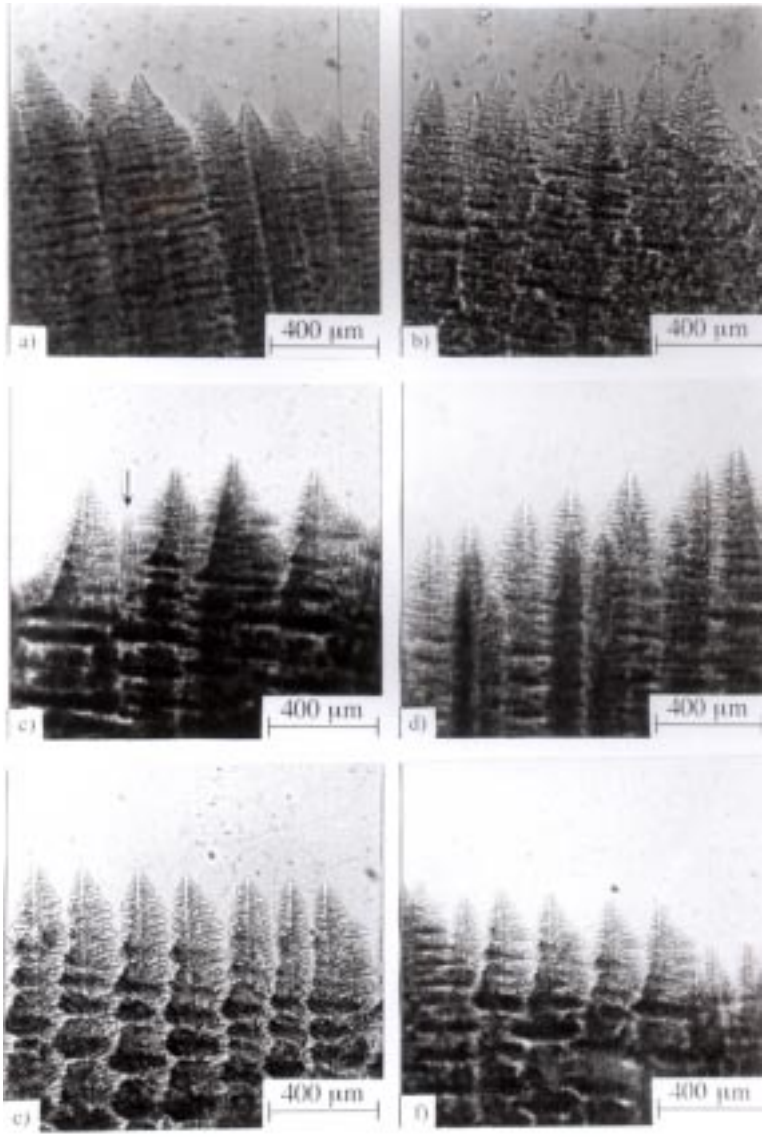

Figure 5. The directional solidification of SCN- 15 wt % Salol system for increasing growth rates in a temperature gradient (G: 69 $^{\circ}$C/cm): a) V:31 x10^{-4} cm/s; b) V:59x10^{-4} cm/s; c) the directional solidification of SCN- 20 wt % Salol system for increasing growth rates in a temperature gradient (G: 26° C/cm), V:14 x10^{-4} cm/s; d) V:32x10^{-4} cm/s e) V:57 x10^{-4} cm/s; f) V:96 x10^{-4} cm/s.

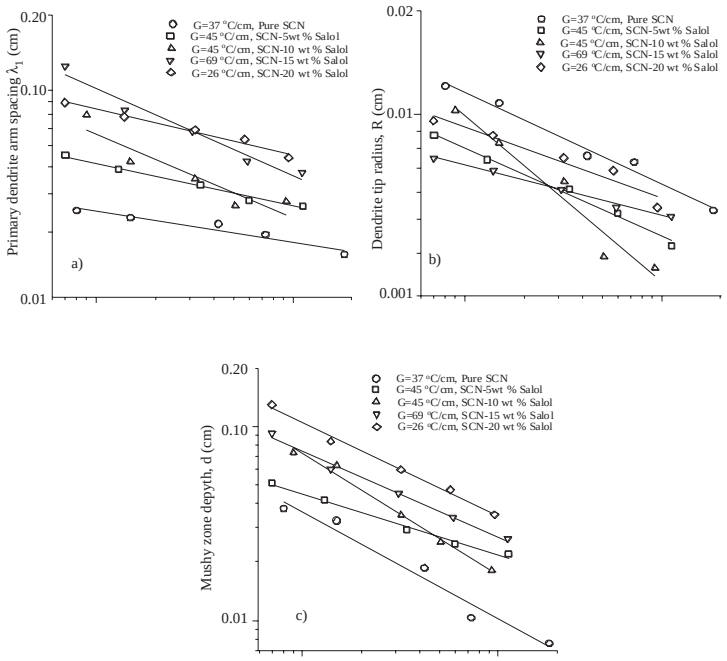

Figure 6. a) The plot of log λ_1 versus logV for each composition. b) The plot of log R versus logV for each composition. c) The plot log d versus log V for each composition.

The exponent values of λ_1, R and d for pure SCN system were found to be -0.14, -0.26 and -0.55, respectively, for five different growth rates spanning 8−183 x10^{-4} cm /s in a temperature gradient of 37 $^{\circ}$C/cm. In this case, d has the maximum exponent value and λ_1 has the minimum value. The exponent values of λ_1, R and d for SCN of 5 wt.% Salol system were found to be -0.19, -0.25 and –0.31, respectively, for five different growth rates spanning 7−113 x10^{-4} cm/s in a temperature gradient of 45 $^{\circ}$C/cm. In this case, d has also the maximum value and λ_1 also has the minimum value. The exponent values of λ_1, R and d for SCN of 10 wt. % Salol system were found to be -0.39, -0.48 and -0.63, respectively, for five different growth rates spanning 9−93 x10^{-4} cm /s in a temperature gradient of 45 $^{\circ}$C/cm. In this case, d has also the maximum exponent value but for this alloys R has the minimum value. The exponent values of λ_1, R and d for SCN -15 wt. % Salol system were found to be -0.40 , -0.15 and -0.44, respectively for five different growth rates spanning 7−112 x10^{-4} cm /s in a temperature gradient of 69 $^{\circ}$C/cm. In this case, d has also the maximum exponent value and R has the minimum value. The exponent values of λ_1, R and d for SCN –20 wt. % Salol system were found to be -0.21 , -0.21 and -0.48, respectively, for five different growth rates spanning 7−96x10^{-4} cm /s in a temperature gradient of 26 $^{\circ}$C/cm. In this case, d has the maximum exponent value and λ_1 and R have the same value. As can be seen from Tables 1 and 2 the differences between the exponent values of λ_1 and R is larger at the high temperature gradient (69 $^{\circ}$C/cm

) and its is zero at the low temperature gradient (26 $^{\circ}$C/cm). From the experimental results, it can be concluded that the temperature gradient and growth rate more affect on the microsucture parameters than the composition of alloys.

As can be seen from Table1, the statistical error in the measurements of λ_1 is 10 %. As can be seen from Figure 5(c) some dendrite trunks disappeared due to competitive growth during the solidification and this leads to a large value for λ_1. The statistical error in the measurements of d is again 10 % . The errors in the measurements of d come from the dendrite tips which were not at the same position due to competitive growth during the solidification, as shown in Figure 5 (a-d) and the dendrite roots were not observed clearly due to the secondary arms growing towards each other at the root of the dendrite. The statistical error in the measurements of R is 6 % and the error come from making a circular fit to a paraboloid-shaped tip.

The average values of λ_1/ R ratios for the SCN-5 wt % salol, SCN-10 wt % salol and SCN-20 wt % salol systems were found to be 5.48, 5.78 and 7.94, respectively, and they seem to be constant. The ratio λ_1/ R increases as growth rate increases in the pure SCN system, because the dependence of the dendrite tip radius on the growth rate is greater than the primary dendrite arm spacing. But the values of λ_1/ R for the SCN 15 wt % salol system decreases as growth rate increases. This happens because, dependence of the primary dendrite arm spacing on the growth rate is more than the dendrite tip radius

The average values of λ_1/ d ratios in the SCN-5 wt. % salol, SCN-10 wt. % salol and SCN-15 wt % salol systems were found to be 1.30, 0.93 and 1.29, respectively, and they seem to be constant. The ratios of λ_1/ d increases as growth rate increases in the pure SCN and SCN-20 wt. % salol systems, because of the dependence of the mushy zone depth on the growth rate is more than the primary dendrite arm spacing.

The average values of R/ d ratios for the SCN-5 wt. % salol and SCN-10 wt. % salol systems were found to be 0.19 and 0.16, respectively, and they seem to be constant. The ratios of R/ d increases as growth rate increases in the pure SCN, SCN-15 wt. % salol and SCN-20 wt. % salol systems, because of the dependence of the mushy zone depth on the growth rate is more than the dendrite tip radius.

From the experimental results it can be concluded that the ratios of the microstructure parameters for different compositions differ from each other. Therefore the composition of alloys plays an important role in the ratios of the microstructure parameters.

5. Conclusions

The change in microstructure parameters (λ_1, R and d) with respect to the solidification parameters (C_o, V and G) for five different growth rates and compositions (pure SCN, SCN -5, 10, 15 and 20 wt. % salol) were investigated and the relationships between them were obtained by linear regression analysis. It was seen that the values of λ_1, R and d decreases as the values of V increase in a temperature gradient.

Table 3. A comparison of the experimental results of the structure parameters (λ_1, R,) with previous works.

System	Temperature Gradient ($^{\circ}$C / cm)	Growth Rate x10^{-4}(cm/s)	Relationships	Refs.
Pure Scn	37	8-183	$\lambda_1 = k_1 V^{-0.14}$	Present work
			$R= k_2 V^{-0.26}$	Present work
			$d =k_3 V^{-0.55}$	Present work
SCN- 5 wt.% Salol	45	7-113	$\lambda_1 = k_4 V^{-0.19}$	Present work
			$R= k_5 V^{-0.25}$	Present work
			$d =k_6 V^{-0.31}$	Present work
SCN- 10wt. % Salol	45	Eyl-93	$\lambda_1 = k_7 V^{-0.39}$	Present work
			$R= k_8 V^{-0.48}$	Present work
			$d =k_9 V^{-0.63}$	Present work
SCN- 15wt. % Salol	69	7-112	$\lambda_1 = k_{10} V^{-0.40}$	Present work
			$R= k_{11} V^{-0.15}$	Present work
			$d =k_{12} V^{-0.44}$	Present work
SCN- 20wt. % Salol	26	Tem-96	$\lambda_1 = k_{13} V^{-0.21}$	Present work
			$R= k_{14} V^{-0.21}$	Present work
			$d =k_{15} V^{-0.48}$	Present work
KCl-5mole% CsCl	30	13-130	$\lambda_1 \propto V^{-0.42}$	[7]
KCl-5mole% CsCl	30	May-52	$\lambda_1 \propto V^{-0.53}$	[7]
SCN-13 wt.% ACE	20	7-Kas	$\lambda_1 \propto V^{-0.58}$	[8]
Cbr_4	70	7-100	$\lambda_1 \propto V^{-0.55}$	[9]
SCN-25wt.% ETH	48	Mar-54	$\lambda_1 = 470\ V^{-0.42}$	[10]
SCN-2.5wt.% Benzil	16-95	56-92	$\lambda_1 = k\ G^{-0.50}\ V^{-0.25}$	[11]
SCN-(0.15-5)wt.% ACE	38	48-225	$\lambda_1 = k\ G^{-0.50}\ V^{-0.25}$	[11]
SCN-1.4wt.% Water	62	140	$\lambda_1 \propto G^{-0.50}$	[12]
Salol	54	May-75	$\lambda_1 \propto k(G\ V)^{-0.50}$	[13]
SCN-(0.001-0.004)mole% Salol	60-150	60-160	$\lambda_1 = 0.16\ G^{-1/3}\ V^{-1/3} X_o^{--1/3}$	[14]
SCN-(0.001-0.004)mole% ACE	60-150	60-160	$\lambda_1 = 0.17\ G^{-1/3}\ V^{-1/3} X_o^{--1/3}$	[14]
SCN-(0.001-0.004)mole% ETH	60-180	60-160	$\lambda_1 = 0.25\ G^{-1/3}\ V^{-1/3} X_o^{--1/3}$	[14]
Cbr_4-10.5wt.% C_2Cl	30	0.1-100	$R \propto V^{-0.53}$	[15]
Cbr_4-7.9wt.% C_2Cl	30	0.1-100	$R \propto V^{-0.47}$	[15]
PVA-0.82wt.% ETH	Eyl-23	0.3-80	$R \propto V^{-0.54}$	[16]
SCN-1.3 wt.% ACE	16-97	1.6-250	$R \propto V^{-0.53}$	[17]
SCN-2 wt.% Water	24-33	0.8-105	$R \propto V^{-0.43}$	[18]
Pure PVA	16-48	6.7-85.8	$\lambda_1 = kV^{-0.32}$	[19]
			$R=kV^{-050}$	
			$d=kV^{-0.45}$	

SCN : Succinonitrile , ACE : Acetone, ETH: Ethanol PVA : Pivalic Acid

A comparison of the present work with previous works is shown in Table 3. As can be seen from Table 3, the exponent values for λ_1, and R, change between -0.25 and -0.58, -0.43 and -0.54 range, respectively, according to composition of alloys in the literature. The results obtained in present work are in good agreement with previous works [7,10,11-18].

In the present work, it was shown that the microstructure parameters can be controlled by change of the solidification parameters. This is very important factor for metallic materials because of the mechanical properties of the metallic materials depend on the microstructure parameters [20-24].

References

[1] S.C. Huang, Ph. D. Thesis, Department of Materials Engineering, Rensselaer Polytechnic Institute, Troy, NY, 1979

[2] M. Chopra, Ph. D. Thesis, Department of Materials Engineering, Rensselaer Polytechnic Institute, Troy, NY, 1984

[3] R.J. Schaefer and M.E. Glicksman, *in modeling of casting and welding process*, (T.M.S.-AIME, Warendale, PA, 1981) p.55

[4] K.A. Jackson and J.D.Hunt, *Acta Metall.* **13**, (1965) 1212

[5] M.E. Glicksman , *Solidification*, (American Society For Metals, Ohio, 1971) p.155

[6] B. Bayender, N. Maraşlı, E. Çadırlı, H. Şişman and M. Gündüz, *Journal of Crystal Growth*, **194**, (1998) 119

[7] W. Schmidbauer, T. Wilke and W. Asmuss, *Journal of Crystal Growth,* **128**, (1993) 240.

[8] S. H. Han and R. Trivedi, *Acta Metall.* **42**, (1994) 25

[9] S. De Cheveigne, C.Guthman and M. M Lebrun, *Journal of Crystal Growth,* **73**, (1985) 242

[10] W. Huang, X. Geying and Y.Zhou, *Journal of Crystal Growth* **134** (1993) 105

[11] M.A. Taha, *Metall. Sci.* **1**, (1979) 9

[12] R.N. Grugel and Y.Zhou, *Metall. Trans.* **20A**, (1989) 969

[13] N. Dey and J.A. Sekhar, *Acta Metall,* **41**, (1993) 409

[14] L. X. Liu and J.S. Kirkaldy, *Journal of Crystal Growth,* **140**, (1994) 115

[15] V. Seetharaman, L.M. Fabrietti and R. Trivedi, *Metall Trans.* **20A**, (1989) 2567

[16] R. Trivedi and J.T. Mason, *Metall Trans.* **22A**, (1991) 235

[17] H. Esaka and W. Kurz, *Journal of Crystal Growth,* **72**, (1985) 578

[18] J.S. Langer and H. Muller-Krumbhaar, *Acta Metall.* **26**, (1978) 1681

[19] E. Çadırlı, N. Maraşlı, B.Bayender and M. Gündüz, *J. Mat. Sci.*, 3**4**, (1999) 5533

[20] R. Trivedi, *Journal of Crystal Growth*, **48**, (1980) 93

[21] E. R Rubinstein and M. E. Glicksman, *Journal of Crystal Growth*, **112**, (1991) 84

[22] P. Bartolotta, J. Barrett, T. Kelly and R. Smasley, *JOM.*, **May**, (1997) 48

[23] F.Yılmaz, R. Elliott, *J. Mat. Sci.* **24**, (1989) 2065

[24] E. Çadırlı, M. Gündüz, *J. Mat. Process and Tech.*, **97**, (2000) 74